Pulsed EPR Studies of the Binuclear Mn(III)Mn(IV) Center in Catalase from *Thermus thermophilus*†

Anabella Ivancich,*,‡ Vladimir V. Barynin,§ and Jean-Luc Zimmermann*,‡

CEA, Centre d'Etudes de Saclay, DBCM, Section de Bioénergétique, Bât 532, 91191 Gif-sur-Yvette, France, and Institute of Crystallography, Russian Academy of Sciences, Leninsky pr. 59, Moscow 117333, Russia

Received September 21, 1994; Revised Manuscript Received March 13, 1995⊗

ABSTRACT: The nature of possible protein ligands to the binuclear metal core in manganese catalase from *Thermus thermophilus* has been addressed by EPR and ESEEM (pulsed EPR) spectroscopies. The three-pulse ESEEM spectrum of the superoxidized Mn(III)Mn(IV) enzyme obtained at 3429 G shows a frequency pattern with peaks at 0.60, 1.45, 2.06, and 5.03 MHz that is assigned to the magnetic coupling in the exact cancellation regime of one ^{14}N atom that coordinates the Mn dimer, with magnetic parameters $e^2Qq = 2.34$ MHz, $\eta = 0.51$, and $A_{iso} = 2.45$ MHz. When the enzyme is chemically modified by reductive methylation, dramatic effects are detected both in the CW-EPR spectrum and in the ESEEM data. Spectral simulations of the CW-EPR signal suggest that the alterations in the spectra are related to the properties of the hyperfine coupling tensors of the Mn ions and of the g tensor, which changes from axial symmetry ($|g_{\parallel} - g_{\perp}| = 0.018$) in the untreated catalase to a nearly isotropic symmetry ($|g_{\parallel} - g_{\perp}| = 0.002$) in the modified enzyme. The three-pulse ESEEM spectrum of the catalase is also completely altered after the reductive methylation, with a rather different frequency pattern at 1.57, 2.35, 3.88, and 6.00 MHz. These data are interpreted as indicating that the hyperfine interaction from the coupled ^{14}N donor is profoundly modified by the methylation treatment, changing from $A_{iso} = 2.45$ MHz to a larger value. The spectra are compared with ESEEM data obtained on two polynuclear Mn systems with ^{14}N donors: the Mn cluster of Photosystem II inhibited by $^{14}NH_4Cl$, and the model compound $[Mn_2(bipy)_4(\mu\text{-}O)_2](ClO_4)_3$. It is found that the ESEEM data measured on the untreated Mn(III)Mn(IV) catalase resemble those on the Photosystem II manganese site, suggesting that the coupled ^{14}N coordinates the Mn dimer in an analogous fashion. By analogy to the mode of binding of ammonia in Photosystem II proposed by Britt et al. [Britt, R. D., Zimmermann, J. L., Sauer, K., & Klein, M. P. (1989) *J. Am. Chem. Soc. 111,* 3522−3532], it is proposed that a ^{14}N atom bridges the two Mn ions in Mn(III)Mn(IV) catalase. By contrast, comparison of the data obtained on the methylated enzyme with those on the model compound suggests that the ^{14}N couplings are similar in both systems; this is indicative of a terminal ^{14}N ligand in the modified catalase. The analysis of the changes in the amino acid composition of the enzyme that is induced by the reductive methylation indicates that the amino acid side chain that is proposed to bridge the two metal ions in Mn(III)Mn(IV) catalase is most probably the ϵ-amino group of a lysine residue.

Catalase enzymes (H_2O_2:H_2O_2 oxidoreductase; EC 1.11.1.6) promote the catalytic disproportionation of hydrogen peroxide, a toxic molecule produced by aerobic metabolism in all aerobic cells, to water and molecular oxygen (Deisseroth & Dounce, 1970; Schonbaum & Chance, 1976; Larson & Pecoraro, 1992; Penner-Hahn, 1992). The majority of catalase enzymes isolated from different organisms contain a heme prosthetic group in the active site, and their three-dimensional structure has been solved to atomic resolution by X-ray crystallography (Murthy et al., 1981; Melik-Adamyan et al., 1986; Murshudov et al., 1992). Much less characterized, however, is another group of catalase enzymes that have been identified and shown to contain manganese. These include catalase from the bacteria *Lactobacillus plantarum* (Kono & Fridovitch, 1983), *Thermoleophilum album* (Algood & Perry, 1986), and *Thermus thermophilus* (Barynin & Grebenko, 1986).

Manganese catalase isolated from *T. thermophilus* is a 210 kDa protein containing six identical subunits, with two manganese ions per subunit (Vainshtein et al., 1985; Barynin et al., 1986). The crystal structure at 3.0 Å resolution shows two metal ions which are separated by ca. 3.6 Å and embedded in four antiparallel α-helices (Barynin et al., 1986). However, a refined structure based on the amino acid sequence of the enzyme, which would enable us to assign the amino acid residues and as a consequence to identify possible ligands to the catalytic site, is still not available. EPR[1] spectroscopy at low temperature has been successfully

† A.I. gratefully acknowledges the postdoctoral fellowship from CONICET (Rep. Argentina) and, for the early part of this work, a C.T.E. contract from CEA-Saclay (France). Partial support from Fundación Antorchas (Rep. Argentina) is also acknowledged.

* Authors to whom correspondence should be addressed. Fax: +33 1 6908 8717; E-mail: zimmermann@dsvidf.cea.fr.

‡ Centre d'Etudes de Saclay.

§ Russian Academy of Sciences.

⊗ Abstract published in *Advance ACS Abstracts,* May 1, 1995.

[1] Abbreviations: EPR, electron paramagnetic resonance, or, equivalently, electron spin resonance or ESR; CW, continuous wave; ESEEM, electron spin echo envelope modulation; ENDOR, electron nuclear double resonance; EXAFS, Extended X-ray absorption fine structure; FT, Fourier transform; NQI, nuclear quadrupole interaction; HPLC, high performance liquid chromatography; MCD, Magnetic Circular Dichroism; cyclam, 1,4,8,11-tetraazacyclotetradecane; tmpa, tris(2-methylpyridyl)amine; bipy, 2,2′-bipyridine; PTC, phenylthiocarbamyl; PSII, Photosystem II.

0006-2960/95/0434-6628$09.00/0

used to study the Mn site in frozen solutions of catalase. EPR signals assigned to three possible oxidation states of the Mn dimer (Mn(II)Mn(II), Mn(II)Mn(III), and Mn(III)-Mn(IV)) were reported and characterized (Khangulov et al., 1990a,b). The EPR signals originate from the exchange coupling between the two Mn ions. In particular, relatively strong exchange coupling between the two Mn ions in the oxidized (Mn(II)Mn(III)) and superoxidized (Mn(III)Mn(IV)) states of catalase produces well isolated $S = {}^1/_2$ ground state doublets, with resolved hyperfine couplings from the two ^{55}Mn nuclei that lead to the detection of multiline EPR signals with 16 major hyperfine lines. The EPR parameters obtained from simulations of the EPR spectra (Zheng et al., 1994) are typical for Mn(III)Mn(IV) dimers bridged by μ-oxo and μ-carboxylato ligands. A multiline EPR signal from the superoxidized state has also been reported in the *L. plantarum* catalase, and the signal was also interpreted in terms of a dimer of manganese ions (Fronko et al., 1988), with EPR parameters very close to those of the *T. thermophilus* enzyme (Haddy et al., 1994).

Structural information on the metal site of the *L. plantarum* catalase was also obtained by EXAFS spectroscopy (Waldo et al., 1992). A Mn···Mn distance of 2.67 Å was identified for the superoxidized state of the enzyme. This result was taken as evidence for the existence of two μ-oxo bridges between the Mn(III) and the Mn(IV) ions, probably with an additional bridging ligand such as a μ-carboxylato (Waldo et al., 1992). This result is consistent with the observation of a 16-line EPR signal for the Mn(III)Mn(IV) state of the catalase from both organisms.

Possible structural models of the catalytic site of *T. thermophilus* have been proposed based on ESEEM (Dikanov et al., 1988) and ENDOR (Khangulov et al., 1993) spectroscopic results. The existence of a nitrogen nucleus that is weakly coupled to the Mn cluster was derived from the ESEEM results, and this was assigned to the remote nitrogen of a histidine ligand (Dikanov et al., 1988). In the ENDOR spectra, however, no signal was detected that could be assigned to ^{14}N nuclei frequencies (Khangulov et al., 1993). By contrast, relatively large ^{14}N ENDOR signals could be detected in the model compound $[Mn_2(bipy)_4(\mu\text{-}O)_2](ClO_4)_3$ in which each manganese ion possesses a N_4O_2 donor set (Khangulov et al., 1993). The original interpretation of the ESEEM results was challenged, and both sets of data were interpreted as indicating either a nonbonding nitrogen nucleus that is hydrogen bonded to an oxo ligand, or a nitrogen nucleus directly bonded to a Mn ion (Khangulov et al., 1993).

Taken together, the structural data that are available from the X-ray crystallography and the results of the different spectroscopic studies described above still provide a limited picture on the binuclear Mn site responsible for catalysis in *T. thermophilus* catalase. In particular, the exact nature of the bridging atoms between the Mn is still unknown, and the amino acid residues that are located near the binding site of the Mn ions are not identified, particularly those involved as ligands to the metals. In addition, the difference mentioned above in the ENDOR data of the Mn site for the catalase enzyme, and for the model compound $[Mn_2(bipy)_4(\mu\text{-}O)_2](ClO_4)_3$, is puzzling, as is the different coupling regime for the nitrogen ligand evidenced by the ESEEM data reported for the two metal sites (Britt, 1988; Dikanov et al., 1988). These differences suggest that the magnetic properties of the nitrogen ligands to the Mn dimers in catalase and $[Mn_2(bipy)_4(\mu\text{-}O)_2](ClO_4)_3$ are different, and hence the nature of the nitrogenous ligand in Mn catalase may not be a histidine imidazole, as has been proposed earlier (Dikanov et al., 1988).

ESEEM spectroscopy is a powerful pulsed EPR technique that can detect weak hyperfine couplings in paramagnetic sites (Kevan, 1990). In particular, weak anisotropic superhyperfine couplings arising from neighboring ^{14}N nuclei in paramagnetic metal proteins can be resolved, that can originate from nearby nitrogenous ligands, or nitrogen-containing substrates or inhibitors that bind to the metal site. In manganese redox enzymes, ESEEM spectroscopy has been successfully applied to characterize the tetranuclear Mn site responsible for oxygen evolution in Photosystem II (Britt et al., 1989; DeRose et al., 1991; Zimmermann et al., 1993). In the first study, direct measurements of the nuclear quadrupole interaction (NQI) parameters of the ^{14}N atom in Photosystem II inhibited by $^{14}NH_4Cl$ were made, and their analysis led to the conclusion that the ammonia molecule binds as an amido bridge between two Mn ions (Britt et al., 1989).

In the present study, an extensive characterization of the Mn(III)Mn(IV) state of manganese catalase by EPR and ESEEM spectroscopy is reported. A nitrogen nucleus that is weakly coupled to the Mn spin is detected by ESEEM, confirming the earlier data by Dikanov et al. (1988). The magnetic parameters of this ^{14}N nucleus are obtained, and these are compared with those derived from the ESEEM spectra of $[Mn_2(bipy)_4(\mu\text{-}O)_2](ClO_4)_3$ and also from the spectra of the Mn tetranuclear complex of Photosystem II inhibited by $^{14}NH_4Cl$ (Britt et al., 1989). Complementary information on the nature of the nitrogenous ligand responsible for the detected ESEEM signals is obtained by chemical modification of catalase and by spectral simulations of the modified multiline EPR signal. From this combined information it is proposed that an unprecedented ϵ-amino group from a lysine residue bridges the two manganese ions in Mn(III)Mn(IV) catalase. The relevance of this result with respect to the mechanism of the enzyme proposed in the literature is discussed.

MATERIALS AND METHODS

Isolation and purification of manganese catalase from *T. thermophilus* were performed as previously described (Barynin & Grebenko, 1986), and the enzyme was stored as a precipitate in 50% saturated ammonium sulfate. Concentration of samples was determined spectrophotometrically (Shimadzu, UV-160A) by using the absorption at 280 nm ($\epsilon = 0.95$ mg^{-1} cm^2; Barynin & Grebenko, 1986), and before further use the precipitate was dialyzed against 10 mM potassium phosphate buffer, pH = 6.8. Manganese catalase in the superoxidized state Mn(III)Mn(IV) was prepared by buffer exchange against 5 mM KIO_4 (Khangulov et al., 1990a), and the final oxidation state of the sample was verified by EPR spectroscopy (Khangulov et al., 1990b). Typical EPR samples contained ca. 1.5 mg/mL protein and gave a 16-line multiline EPR signal identical to those published in the literature for Mn(III)Mn(IV) catalase (Khangulov et al., 1990b; Zheng et al., 1994). Typical samples for pulsed EPR spectroscopy were prepared in the same manner, except that the protein concentration was larger (ca. 2.6 mg/mL).

Reductive methylation of the amino groups of the catalase was done by using the method described in Berger et al. (1984), and references therein. Briefly, formaldehyde and $NaBH_3CN$ were directly added to the EPR sample containing superoxidized catalase; the concentrations were sufficient to potentially methylate all the amino side chains present in the enzyme (the guanidinium group of arginine, the imidazole of histidine, and the primary amine of lysine). This was based on the results of the amino acid composition of the enzyme (12 Arg, 9 His, and 21 Lys; V. V. Barynin, unpublished results). The sample was then incubated at 35 °C for 45 min and frozen to 77 K before the changes induced by the methylation were characterized. EPR and ESEEM measurements were also performed after additional periods of incubation at 35 °C of the sample (see the Results section).

Amino acid analyses of the catalase samples were performed using an Applied Biosystems analyser; hydrolysis of the enzyme samples was performed in 6 N HCl *in vacuo* at 110 °C for a period of 22 h. Phenylthiocarbamyl (PTC) amino acid derivatives were obtained by mixing the hydrolyzed sample with phenyl isothiocyanate (Bidlingmeyer et al., 1984) and were identified by comparison with the HPLC profile of the mixture of standards of free amino acids with PTC. For the identification of the PTC derivatives of methylated lysine, poly(L-lysine hydrochloride) (Sigma) was treated in the same conditions as the catalase sample.

The model compound $[Mn_2(bipy)_4(\mu\text{-}O)_2](ClO_4)_3$ was prepared as already described (Cooper & Calvin, 1977) and was kindly provided by Dr. V. K. Yachandra (Lawrence Berkeley Laboratory, Berkeley, CA). For EPR and pulsed EPR measurements the compound was dissolved (1 mM) in CH_3CN/CH_2Cl_2 in a 1:1 ratio, and the sample was immediately frozen in liquid N_2 before EPR and pulsed EPR data were collected.

Photosystem II membranes evolving oxygen were prepared from spinach leaves, and further inhibition by NH_4Cl was done as already described (Britt et al., 1989). The extent of inhibition was verified by the appearance of the characteristic EPR multiline signal originating from the binding of ammonia to the Mn tetramer (Britt et al., 1989).

CW-EPR spectra were recorded at X-band with a Bruker 200-D spectrometer using a standard TE_{102} cavity equipped with a liquid helium cryostat (Oxford Instruments). A microwave frequency counter (Hewlett Packard 5350B) and an NMR gaussmeter (Bruker ERO35M) were used for precise measurements of the frequency and magnetic field values. This proved to be necessary to extract accurate EPR parameters from the simulations of the spectra. The simulations of the EPR spectra shown in this work were done using a computer program that calculates the hyperfine coupling contributions as perturbations of the electronic Zeeman interaction to the second order (see Bonvoisin et al., 1992).

For ESEEM experiments, a Bruker ER 380 pulsed EPR spectrometer equipped with a dielectric resonator that allows adjustment of the loaded Q value was employed. Instrument deadtimes thus obtained were typically 100 ns. All measurements reported in this study were performed at 4.2 K using an Oxford Instruments liquid helium immersion Dewar. The ESEEM signals reported in this study were measured as the amplitude of the stimulated echo produced by a sequence of three resonant $\pi/2$ microwave pulses, when the interpulse time T separating the second and the third pulses is varied, and the first interpulse time τ is kept fixed. Appropriate pulse phase cycling was done as described in Fauth et al. (1986) to eliminate contributions from secondary echoes to the three-pulse echo envelope. The τ values used in this study were chosen as twice the inverse of the proton Larmor frequency for the external magnetic field strength, so that modulations due to weakly coupled protons were suppressed in the stimulated echo signal (Mims & Peisach, 1981).

In some experiments, echo-detected EPR spectra were recorded, in which the amplitude of a simple Hahn echo ($(\pi/2)-\tau-\pi-\tau-$echo) was measured while incrementing the magnetic field stepwise on successive spin-echo generating pulse sequence iterations. In this way, an EPR absorption-like spectrum was obtained, that could be compared after numerical differentiation to the field-modulated EPR line obtained in the conventional CW-EPR mode.

Fourier transformation of the ESEEM data sets was performed using a program written in the laboratory at CEA; it performs the FT analysis using a modified deadtime reconstruction algorithm (Mims, 1984). This program is based on the FORTRAN code kindly made available to us by Prof. John McCracken (Michigan State University).

RESULTS

Three-pulse ESEEM data on superoxidized Mn(III)Mn(IV) catalase have been reported by Dikanov et al. (1988). The envelope modulation is very characteristic and gives a unique frequency pattern after Fourier transformation. Data obtained under similar conditions for the enzyme used in the present study are shown in Figure 1 (panel A: time domain data; panel B: Fourier transform). As mentioned by Dikanov et al. (1988), this pattern of frequencies with three sharp low frequency peaks designated ν_0, ν_-, and ν_+, verifying $\nu_+ = \nu_- + \nu_0$, and a broader component at higher frequencies (5.03 MHz in Figure 1B) is typical of a system with nuclear spin $I = 1$ coupled to the electronic spin, in the coupling regime known as the exact cancellation limit (Flanagan & Singel, 1987). In biological samples, anisotropic hyperfine couplings giving rise to such a characteristic ESEEM pattern can be assigned to couplings with ^{14}N nuclei with reasonably good confidence, and thus the peaks in the Fourier transform shown in Figure 1B arise from a nitrogen nucleus coupled to the spin of the Mn(III)Mn(IV) moiety (Dikanov et al., 1988). Interpretation of ESEEM spectra in the regime of exact cancellation has been particularly well characterized in systems with Cu(II) ($S = {}^1/_2$) coordinated with imidazole or histidine ligands, such as numerous model compounds and also Cu(II) proteins (Mims & Peisach, 1989). ESEEM spectra for other metal centers in proteins that show the typical components of the exact cancellation regime have also been interpreted in terms of a coupled ^{14}N nucleus. These include the Ni(II) center of a hydrogenase from *Methanobacterium thermoautotrophicum* (Tan et al., 1984) and a Fe-S center from fumarate reductase from *Escherichia coli* (Cammack et al., 1988). For Cu(II) coordinated with imidazole ligands, it has been well established that the magnitude of the hyperfine coupling of the nitrogen atom that is coordinated to the Cu(II) ion is too large to be observed by ESEEM, and that the nitrogen frequencies observed in the ESEEM arise from the *remote* nitrogen of the imidazole moiety (Mims & Peisach, 1978). For this remote nitrogen, the nuclear Zeeman and hyperfine interactions add in one electron spin manifold (the β manifold), whereas they

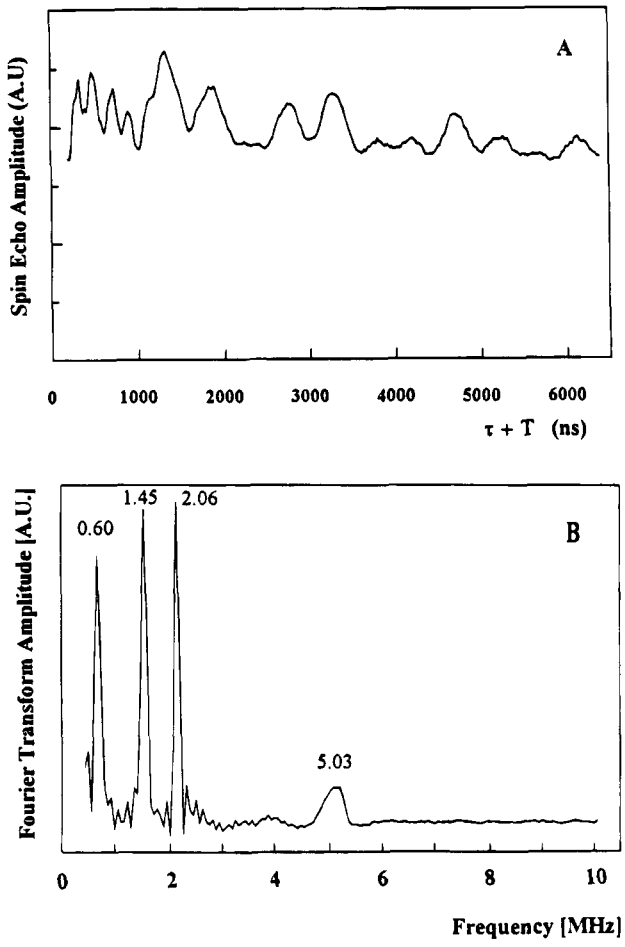

FIGURE 1: Three-pulse ESEEM signal (panel A) and Fourier transform (panel B) for a Mn(III)Mn(IV) catalase sample. The stimulated echo was monitored as a function of the interpulse time $\tau + T$; the data were obtained at a temperature of 4.2 K, a microwave frequency of 9.57 MHz, and a magnetic field of 3429 G. The time interval between spin-echo pulse sets was 1 ms. The interpulse time τ between the first and second pulses was set to 136 ns., corresponding to approximately twice the Larmor period of weakly coupled protons. The observed ^{14}N ESEEM frequencies are 0.60, 1.45, 2.06, and 5.03 MHz.

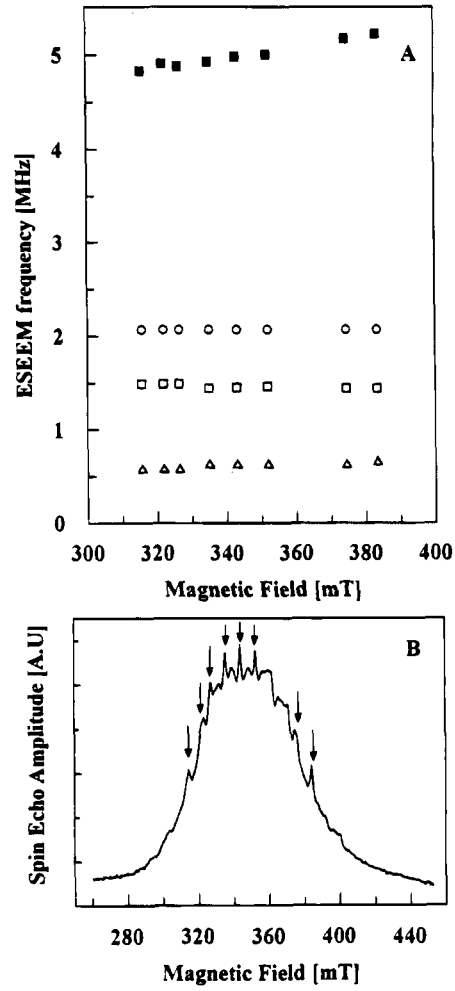

FIGURE 2: Magnetic field dependence of the four ^{14}N ESEEM frequencies, ν_0 (open triangles), ν_- (open squares), ν_+ (open circles), and ν_{dq} (filled squares), for the Mn(III)Mn(IV) catalase sample (Panel A). The experimental conditions were the same as those used in Figure 1. The magnetic field values were chosen from the best resolved hyperfine lines (indicated by arrows) in the echo-detected EPR spectrum (panel B) obtained with $\tau = 200$ ns.

subtract and cancel in the second manifold (the α manifold). In this case, called the exact cancellation regime, the three lowest ESEEM frequencies ν_0, ν_-, and ν_+ are a direct measurement of the nuclear quadrupole interaction (NQI) frequencies, and these can be related to the geometry around the nitrogen (Jiang et al., 1990). The fourth and broader line in Figure 1B can be assigned to a $\Delta M = 2$ transition in the β manifold and is referred to as the "double quantum" line. Consequently, the observation of such a frequency pattern in the ESEEM of a Cu(II) protein is a demonstration of the existence of a histidine ligand; these properties have been used to identify histidine imidazole ligands in a number of Cu(II) proteins, where the coordination of the copper was unknown (Mims & Peisach, 1989).

On the basis of these properties, Dikanov et al. (1988) proposed a similar interpretation for the ESEEM data of Mn(III)Mn(IV) catalase, i.e., the frequencies arise from the interaction of the remote nitrogen of a histidine imidazole that coordinates the Mn dimer. As mentioned above, there is no doubt that such a frequency pattern is reminiscent of a ^{14}N nucleus coupled to the Mn spin in the exact cancellation limit; however, in the present case of Mn catalase, the coupled ^{14}N may not be the remote nitrogen of a histidine ligand, as the hyperfine coupling parameters with ligand atoms are expected to be different for Mn(III) and Mn(IV) compared to Cu(II). In fact, the experiments reported below will lead us to a completely different interpretation with regard to the particular protein amino acid which contains this nitrogen nucleus, as well as its mode of coordination. As complementary ESEEM results on Mn(III)Mn(IV) catalase, Figure 2A shows the magnetic field dependence of the four peaks of the spectrum in Figure 1B. In this experiment, the three-pulse ESEEM signal was recorded at different magnetic field positions throughout the ca. 1200 G wide EPR multiline signal (see Figure 2B). As expected for this coupling regime (Flanagan & Singel, 1987), the three lowest frequencies are virtually independent of the magnetic field strength, whereas the fourth "double quantum" line varies approximately linearly with the magnetic field (Figure 2A). From the frequency values of the NQI lines, one can calculate the quadrupole coupling constant $e^2Qq = 2.34$ MHz, and the asymmetry parameter of the quadrupole tensor $\eta = 0.51$. The isotropic part of the hyperfine coupling constant $A_{iso} = 2.45$ MHz can also be evaluated from the frequency position of the "double quantum" line and the NQI frequencies.

These values are in agreement with those reported by Dikanov et al. (1988), although in the published spectra, the three low frequency lines are broad and the "double quantum" line is not well-defined. As shown by the results in Figure 2A, a pattern of lines similar to that shown in Figure 1B can be measured for magnetic field values covering the entire spectral range of the EPR signal of Mn(III)Mn(IV) catalase, and the value of A_{iso} that can be calculated from these measurements is virtually field independent. This indicates that the degree of anisotropy of the hyperfine interaction is sufficiently weak so that the regime of exact cancellation remains valid over this magnetic field range, and that the hyperfine interaction of the nitrogen nucleus is mostly isotropic. In fact, simulations of the ESEEM spectra should be performed in order to calculate the anisotropic contribution to the hyperfine interaction. Inspection of the spectrum in Figure 1B does not show the presence of intermodulation lines that originate from the combination of the fundamental NQI lines when more than one ^{14}N contributes to the ESEEM (Mims & Peisach, 1989). This indicates that only one nitrogenous ligand is coupled to the Mn(III)Mn(IV) site in catalase. For defining the chemical identity of this nitrogenous ligand, it is worth pointing out that, on the basis of their ENDOR results, Khangulov et al. (1993) proposed an alternative interpretation of the ESEEM results, in that the nitrogen would be directly coordinated to the Mn(III)Mn(IV) dimer, but by no means could be the remote nitrogen of a histidine ligand.

To better understand the mode of coordination of the nitrogenous ligand responsible for the ESEEM spectrum, and to test possible candidates for it, Mn(III)Mn(IV) catalase was subjected to reductive methylation, a treatment that is expected to label accessible amino groups in the protein and involves incubation with formaldehyde and sodium cyanoborohydride. After several successive 45 min incubation periods at 35 °C, the EPR spectrum of catalase was measured and is shown in Figure 3 (trace b), together with the signal obtained for the same sample before the treatment (Figure 3, trace a). The spectrum of the treated enzyme is similar to that before the treatment, with 16 major hyperfine lines centered around $g \cong 2$. This result indicates that the Mn ions are still present as a dimer after the treatment and that their oxidation state is still Mn(III)Mn(IV). Close observation of the spectrum shows however that its overall breadth is somewhat smaller in the treated enzyme (1160 G vs 1175 G) and that marked shifts and splittings of some of the hyperfine lines have been induced by the treatment. For instance, the leftmost hyperfine line is now split into two lines that are separated by ca. 30 G. A similar change is apparent in the high field part of the spectrum. These modifications can be quantitatively characterized by simulations of the EPR spectra. One of the simulations that best reproduces these new features in the EPR spectrum is shown in Figure 3 (trace c), and the g and A tensor component values used for this simulation are listed in Table 1, together with those of related spectra. In particular, the spectrum of the control Mn(III)Mn(IV) catalase could be simulated with almost the same EPR parameters (see Table 1) as those reported by Zheng et al. (1994) and Haddy et al. (1994), resulting in a simulated spectrum which reproduced exactly all the features of the experimental spectrum (data not shown). Table 1 shows that the best fit for the methylated catalase is obtained with $A_\perp = 443.7$ MHz and $A_\parallel = 404.7$ MHz, whereas for the untreated enzyme one obtains $A_\perp = 311.8$ MHz and $A_\parallel = 425.7$ MHz for the hyperfine couplings of the Mn(III) ion. Of particular note is the change in the symmetry of the g tensor. While the g tensor of the Mn(III)Mn(IV) site in the untreated enzyme is markedly anisotropic with $\Delta g = |g_\parallel - g_\perp| = 0.018$, the g tensor that is derived from the simulation of the methylated enzyme is nearly isotropic ($\Delta g = 0.002$). This strongly suggests that the reductive methylation has modified an amino acid that is very close to the Mn dimer site, and that as a consequence of the induced geometrical changes near the manganese site, the electron spin density distribution on the Mn nuclei is perturbed, and the symmetry of the dimer Mn core is altered.

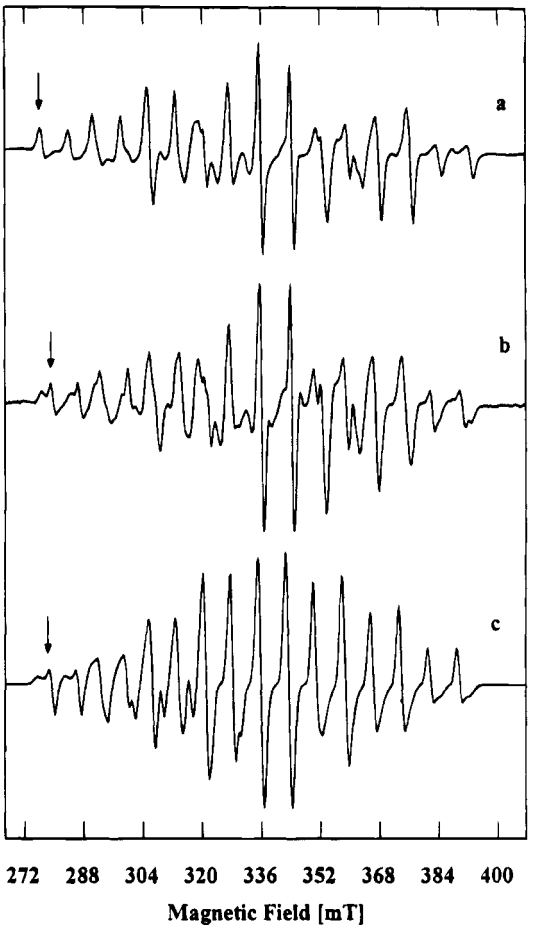

FIGURE 3: Comparison of the CW-EPR spectra of Mn(III)Mn(IV) catalase (trace a), methylated Mn(III)Mn(IV) catalase (trace b), and the best simulation of spectrum b (trace c). The experimental conditions used were the following: temperature, 4.2 K; modulation amplitude, 5 G; microwave power, 2.5 mW.; microwave frequency, 9.42 GHz. The arrows emphasize the shift and splittting of the low frequency features (see Results section) following the methylation procedure.

These CW-EPR results provide information on the changes in the hyperfine couplings from the ^{55}Mn nuclei. The possible changes in the magnetic coupling from the ^{14}N of the nitrogen ligand can be addressed by pulsed EPR. Even more dramatic changes accompany the reductive methylation of the enzyme in the ESEEM spectrum. Figure 4 shows the time domain ESEEM signal (panel A) and the Fourier transform (panel B) measured at 3440 G, after 5 periods of incubation at 35 °C, i.e., in the conditions of Figure 3B. The typical pattern (Figure 1B) of three sharp NQI lines and a fourth broader line has vanished and is replaced by an intense

Table 1: EPR Parameters for Control and Chemically Modified Manganese Catalase[a]

	g		A (MHz)			
			Mn(III) ion		Mn(IV) ion	
	$g_x = g_y$	g_z	$A_x = A_y$	A_z	$A_x = A_y$	A_z
methylated Mn(III)Mn(IV) catalase	2.0040	2.0060	404.7	443.7	209.9	215.8
Mn(III)Mn(IV) catalase	2.0075	1.9900	425.7	311.8	227.8	250.3
Mn(III)Mn(IV) catalase[b]	2.0079	1.9897	424.4	312.1	227.7	250.3

[a] g factor and hyperfine coupling constant values were calculated by using axial approximation for g and A matrices. [b] Data from Haddy et al. (1994), converted from energy units using the following conversion factor: 1 cm^{-1} = 2.9979 × 10^4 MHz.

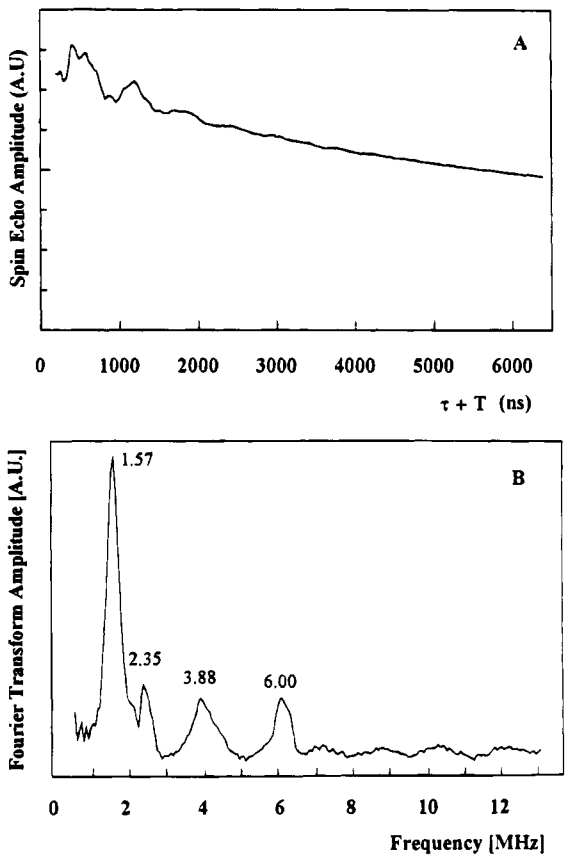

FIGURE 4: Three-pulse ESEEM signal (panel A) and Fourier transform (panel B) for the Mn(III)Mn(IV) catalase sample, treated by reductive methylation. The stimulated echo was monitored as a function of the interpulse time $\tau + T$. The data were recorded at a temperature of 4.2 K, a microwave frequency of 9.61 MHz, a magnetic field of 3440 G, and with a time interval between successive spin-echo pulse sets of 1 ms. The time τ was set to 208 ns, which corresponds to 3 times the Larmor period of weakly coupled protons. The observed ^{14}N ESEEM frequencies are 1.57, 2.35, 3.88, and 6.00 MHz.

frequency component at 1.57 MHz, together with additional lines at 2.35, 3.88, and 6.00 MHz (Figure 4B). This result strongly suggests that the reductive methylation procedure has probably labeled the amino acid responsible for the modulations in Figure 1 and is additional evidence that, in the untreated Mn(III)Mn(IV) catalase, the ESEEM pattern originates from a nitrogenous ligand. The pattern of frequencies for the methylated catalase is much less characteristic than that shown and discussed above for the untreated catalase, and the typical pattern of the exact cancellation regime is not obvious from this spectrum only. An attractive interpretation is that reductive methylation of an amino group that is coordinated to one (or both) manganese ion(s) of the dimer leads to a change in the hyperfine coupling constant and/or the NQI parameters of the amino nitrogen. This in turn would lead to a significant deviation from the exact cancellation regime and consequently a different modulation pattern in the ESEEM spectrum, as is experimentally observed.

To test this hypothesis, ESEEM data were collected for two other polynuclear Mn systems with coordinating nitrogen(s) and that seemed relevant to the present study. The first of these systems is the tetranuclear manganese cluster of Photosystem II inhibited by ammonia. This system has been studied by Britt et al. (1989): the three-pulse ESEEM spectrum showed a pattern of frequencies typical of the exact cancellation regime. In addition, valuable NQI parameters were extracted from the data (e^2Qq = 1.61 MHz and η = 0.59 for H = 3500 G), and from the interpretation of these values it was proposed that the ammonia moiety binds as an amido bridge between two Mn ions of the catalytic cluster. ESEEM data on Photosystem II inhibited by NH_4Cl were collected in this laboratory under conditions that are comparable with those used for the Mn(III)Mn(IV) catalase. The spectrum obtained for a magnetic field of 3660 G is shown in Figure 5A. This spectrum shows three sharp lines at 0.40, 1.04, and 1.46 MHz that are assigned to the NQI frequencies. This is very similar to the data published in the original report, but the significantly improved signal-to-noise ratio of the signal allows the "double quantum" line at 4.74 MHz to be clearly resolved here. Consequently, the value of the isotropic hyperfine coupling constant can be directly evaluated from the three-pulse data alone: A_{iso} = 2.24 MHz for H = 3660 G. The NQI parameters that can be calculated with the data presented here (e^2Qq = 1.67 MHz and η = 0.48) are very close to those reported by Britt et al. (1989). It is interesting at this point to compare the ESEEM data on the ammonia-treated Photosystem II (Figure 5A) with those on the untreated Mn(III)Mn(IV) catalase (Figure 5B) that are recorded under the same experimental conditions, and to emphasize that both show a coupled nitrogen in the exact cancellation regime. The significance of this, as well as the similarity (and also differences) of the corresponding data sets, will be discussed below.

The second Mn system that was studied is the model compound $[Mn_2(bipy)_4(\mu\text{-}O)_2](ClO_4)_3$. This complex is interesting because it is a mixed valence Mn(III)Mn(IV) dimer, just like the metal core of Mn catalase. In addition, each of the two Mn ions has four nitrogen donors from the bipyridyl ligands, and it might be expected that the magnetic coupling between the nitrogen nuclei and the Mn spin is similar to that found for the Mn(III)Mn(IV) catalase. The FT ESEEM spectrum recorded at 3660 G is shown in Figure 5C. The modulations originate from the coupling with the four directly coordinated ^{14}N from the bipyridyl aromatic rings. The frequency pattern shown in Figure 5C is in good

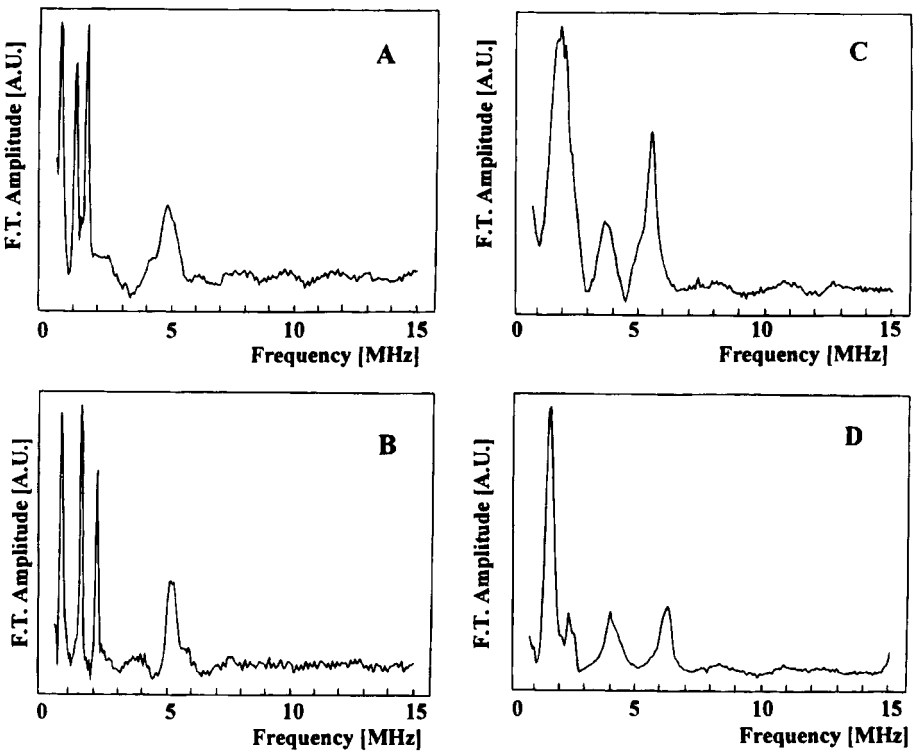

FIGURE 5: Panels A and B show the three-pulse FT-ESEEM spectra obtained with PSII membrane fragments inhibited by ammonia and Mn(III)Mn(IV) catalase, respectively. Peaks at 0.40, 1.04, 1.46, and 4.74 MHz are observed in panel A; and at 0.61, 1.43, 2.06, and 5.10 MHz in Panel B. The magnetic field and τ values used were 3660 G and 192 ns, respectively. Panels C and D show the three-pulse FT-ESEEM spectra of the $[Mn_2(bipy)_4(\mu\text{-}O)_2](ClO4)_3$ model compound and the methylated Mn catalase. Frequencies at 1.92, 2.07, 3.70, and 5.47 MHz (3660 G, τ = 192 ns) are resolved in panel C; and at 1.57, 2.32, 3.96, and 6.23 MHz (3525 G, τ = 200 ns) in panel D.

agreement with that reported by Britt (1988): the main features are a first intense peak at 1.92 MHz and a second at 5.47 MHz, the latter one showing a slight dependence on the external magnetic field strength; a third feature with small relative amplitude appears at 3.70 MHz, that approximately corresponds to twice the value of the lower frequency peak, and thus could be assigned to intermodulation products resulting from multiple ^{14}N nuclei (Mims, 1972). The frequency pattern shown in Figure 5C is not characteristic of the exact cancellation regime, but possible interpretations are given in the Discussion section. However, it is useful to compare it with that obtained under similar conditions for the methylated catalase, and shown in Figure 5D: both spectra show an intense feature at 1.6−1.9 MHz, a line at ca. 3.8 MHz with smaller relative amplitude, and another peak at 5−6 MHz. In addition, the presence of an additional but smaller peak at 2.31 MHz in the spectrum of the modified enzyme may be correlated to unresolved peaks in the broader line at 1.92 MHz of the Mn model compound (Figure 5C).

Regardless of the exact theoretical assignment of the ESEEM frequency features in Figure 5C, and despite the lack of ESEEM data on other polynuclear Mn model compounds with different terminal ligands, the FT ESEEM spectrum of the Mn bipyridyl complex can probably be considered as representative of the couplings from a ^{14}N coordinated to one manganese ion in a Mn(III)Mn(IV) dimer. Further, the strong similarity of this spectrum with that of the methylated catalase (Figure 5D) argues for a similar nitrogen coordination in both the Mn bipyridyl dimer and the Mn dimer in methylated catalase. This strongly suggests that the Mn(III)Mn(IV) unit in the methylated catalase possesses a terminal nitrogen ligand.

Similarly, comparison of the spectra of the untreated catalase (Figure 5B) with that of the $^{14}NH_4Cl$ inhibited Photosystem II (Figure 5A) is suggestive of a rather similar nitrogen coordination in both systems; i.e., the nitrogen ligand bridges two Mn ions. The strong similarity of the NQI parameters for the coupled ^{14}N that are derived from the spectroscopic data in the two systems is a strong support for this interpretation. The asymmetry parameter $\eta = 0.51$ of the ligand ^{14}N in the untreated catalase indicates a significant deviation from the strictly axial field gradient symmetry ($\eta = 0$). As already discussed by Britt et al. (1989), this value of the asymmetry parameter is much higher than that found for model compounds with amino groups as terminal ligands. This suggests that the amino acid that coordinates the Mn(III)Mn(IV) site forms an amido bridge between the two Mn ions. Amino acids with a nitrogen atom that may coordinate the Mn(III)Mn(IV) core as a bridge between the two metal ions include arginine and lysine. After deprotonation, an amino group from the side chain of an arginine or lysine may serve as a bridging ligand between the two metal ions, with a configuration of low electric field gradient symmetry.

As mentioned above, the spectroscopic data on the methylated catalase, and the similarity with those on the Mn bipyridyl dimer, strongly suggest that, after methylation, the ^{14}N donor coordinates the Mn dimer in a terminal position. It is proposed that methylation of the bridging amino group of the Mn(III)Mn(IV) core in catalase causes the disruption of the amido bridge. A nearby donor group from an amino acid or simply a water molecule may replace the ligand that is lost by one of the Mn ions. And consequently, the nitrogen

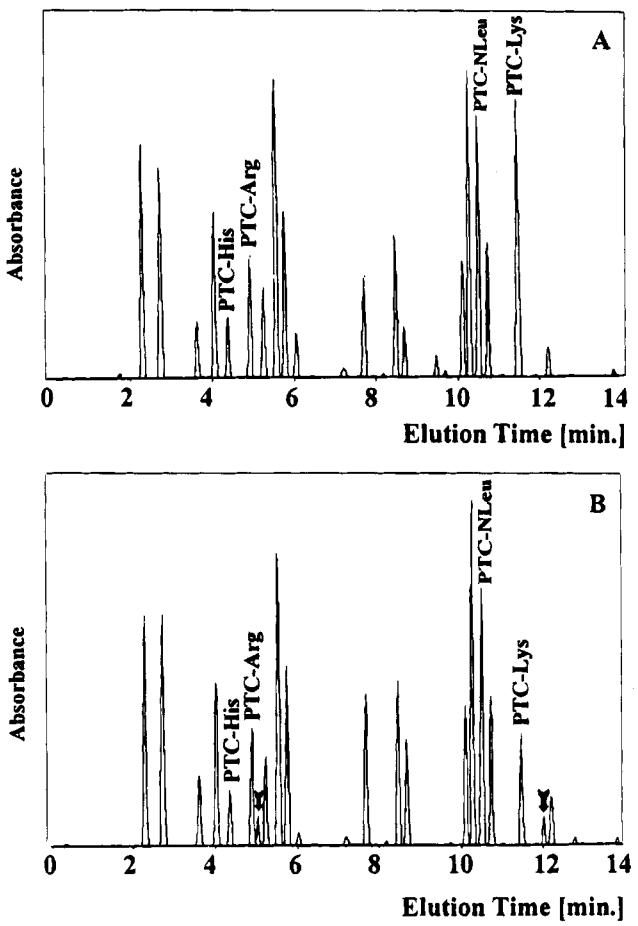

FIGURE 6: HPLC elution profiles of hydrolyzed samples of control (panel A) and methylated (panel B) Mn(III)Mn(IV) catalase. The absorbance of the PTC-amino acid derivatives was measured at 254 nm. The filled downward arrows in panel B show the absorbance peaks for the PTC-methylated lysine derivatives identified in the labeled catalase sample. The peak corresponding to an elution time of 10.50 min is an internal standard (NOR-leucine derivative), and the one at 6.00 min corresponds to a byproduct of the method (DPTU, diphenylthiourea).

donor to the Mn dimer changes from a bridging to a terminal ligand.

To assess the identity of the protein residue that is responsible for the ESEEM pattern and that is proposed to provide a bridging ligand to the Mn(III)Mn(IV) dimer in catalase, and to ascertain and further refine the interpretation given above, the amino acid composition of the enzyme was analyzed before and after the methylation treatment. As mentioned above, incubation of the protein at 35 °C with formaldehyde and cyanoborohydride may induce methylation of protein residues bearing one or several amino groups. These include arginine, lysine, and histidine amino acid side chains. Figure 6 shows the HPLC elution profile obtained for a hydrolyzed sample of Mn catalase before (panel A) and after (panel B) performing the reductive methylation procedure. Comparison of the absorbance peak areas for untreated and modified catalase shows that only 3% of the histidines and 7% of the arginines are modified by the treatment but that approximately 64% of the lysine residues have been methylated. Taken together with the amino acid composition on the Mn catalase of *T. thermophilus* (9 His, 12 Arg, and 21 Lys, V. V. Barynin, unpublished data), these results indicate that 13 Lys, while a maximum amount of 0.3 His and 0.7 Arg ,have been methylated.

In addition, two new peaks (shown with arrows in Figure 6B) are observed in the HPLC profile of the methylated enzyme. These two peaks are assigned to methylated lysine derivatives, as a sample of poly(L-lysine) subjected to the reductive methylation treatment yielded an HPLC profile with two peaks with the same elution times (data not shown). That the product of the methylation yielded two peaks on the HPLC profile has also been observed for other proteins (Means & Feeney, 1968).

These results, together with the spectrocopic data described above, are strong evidence that the nitrogenous ligand to the manganese that is detected by ESEEM spectroscopy originates from the ϵ-amino group of a lysine residue. Both ESEEM spectra of the enzyme before and after methylation show couplings between the nitrogen donor and the Mn, but this coupling is different after substitution of a hydrogen by a methyl group on the amine. It is proposed that, in Mn(III)Mn(IV) catalase, the two Mn ions are bridged by the ϵ-amino group of a lysine residue.

DISCUSSION

The EPR and pulsed EPR spectroscopic results described above on the Mn(III)Mn(IV) catalase, as well as those on the chemically modified enzyme, and the correlation with the results of the amino acid analysis for both cases, provide complementary information that indicates that the ϵ-amino group of a lysine residue forms a bridge between the Mn(III) and the Mn(IV) ions of the dimer.

This interpretation is in contradiction with that provided by Dikanov et al. (1988) who attributed the ESEEM frequency pattern of Mn(III)Mn(IV) catalase to the interaction with the remote nitrogen of a histidine ligand. In fact, this earlier interpretation could not be reconciled with subsequent CW ENDOR data, as the expected frequencies from the directly coordinated ^{14}N of the histidine were absent from the ENDOR spectra (Khangulov et al., 1993). In addition, the hyperfine coupling constant for the coordinated nitrogen of imidazole bound to a metal is expected to be $\cong$20 times larger than that of the remote nitrogen. This is based on pulsed ENDOR and ESEEM data on Cu(II) sites with imidazole ligands (see Thomann & Bernardo, 1993). Thus, if the ^{14}N nucleus detected in the ESEEM of catalase with A_{iso} = 2.45 MHz were the remote nitrogen of the hypothetical histidine ligand, then the coordinated nitrogen would be expected to be coupled with $A_{iso} \cong 49$ MHz. This is clearly incompatible with the EPR data. In fact, LoBrutto et al. (1986) estimated the hyperfine coupling constant for ^{14}N in Mn(II) coordinated with a thiocyanate ligand, $A_{iso} \cong$ 2.7 MHz. Values of A_{iso} for ^{14}N coordinated to Mn(III) or Mn(IV) are expected to be of the same order of magnitude and agree well with the interpretation given in the present study on a coordinated ^{14}N in Mn(III)Mn(IV) catalase. Finally, the results reported here indicate that the nitrogen responsible for the ESEEM can be methylated, but that the nitrogen remains coordinated after methylation of the amine, with concomitant change in the magnetic coupling regime. This rules out histidine as a possible candidate for the nitrogen ligand.[2]

[2] Substitution of the hydrogen by a methyl group on the remote nitrogen of the imidazole is not expected to bring large changes in the hyperfine coupling constant of the coordinated nitrogen so as to change the coupling regime of the latter (see Jiang et al., 1990).

The data indicate that the coupling of the ^{14}N satisfies the conditions of the exact cancellation regime; i.e., the nuclear Zeeman and the hyperfine interactions are on the same order of magnitude ($\nu(^{14}N) = 1.06$ MHz, and $^1/_2A_{iso} = 1.23$ MHz, taking $H = 3429$ G as the approximate field for cancellation). The isotropic part of the hyperfine coupling $A_{iso} = 2.45$ MHz is much smaller than that measured for the ligand ^{14}N in Mn(III)Mn(IV) model compounds by CW ENDOR spectroscopy. Tan et al. (1991) determined $A_{iso} = 11.2$ MHz for the axial pyridine nitrogens in $[Mn_2(tmpa)_2O_2](ClO_4)_3$, and $A_{iso} = 9.2$ MHz for the axial amino nitrogens in $[Mn_2(cyclam)_2O_2](ClO_4)_3$. These coupling constants are as much as 4 times larger than the hyperfine interaction measured for the ^{14}N in catalase. Small hyperfine interactions are not easily detectable by CW ENDOR spectroscopy because the nuclear transition moments are not enhanced by electronic admixture as in the case of large A values (Mims & Peisach, 1981). This situation might explain why no signature from ^{14}N was observed by Khangulov et al. (1993) in the ENDOR spectra obtained on the enzyme, by contrast to the data on the model compound $[Mn_2(bipy)_4(\mu\text{-}O)_2](ClO_4)_3$ that has terminal nitrogen ligands with $A_{iso} \cong 9$ MHz (Khangulov et al., 1993). On the other hand, the electric field gradient of the bonded ^{14}N nuclei in the three Mn(III)Mn(IV) model compounds mentioned above is very close to $e^2Qq = 3.0$ MHz (Tan et al., 1991; Khangulov et al., 1993). The ESEEM data reported in this study indicate that the electric field gradient is also comparable for the coupled nitrogen ligand in Mn(III)Mn(IV) catalase, with $e^2Qq = 2.34$ MHz. This strongly suggests that the differences seen in the ESEEM data for the coupling regime of the ^{14}N in catalase and in $[Mn_2(bipy)_4(\mu\text{-}O)_2](ClO_4)_3$ (Khangulov et al., 1993) arise from the large difference in the isotropic coupling constant. With an estimated $A_{iso} \cong 9$ MHz, and $\nu(^{14}N) = 1.08$ MHz at 3500 G, the regime of exact cancellation is obviously not adequate to describe the ESEEM data of the $[Mn_2(bipy)_4(\mu\text{-}O)_2](ClO_4)_3$ model compound.

By contrast to the typical pattern of a coupled ^{14}N in the exact cancellation limit, an exact theoretical assignment of the ESEEM frequency features observed for a terminal ^{14}N donor coupled to a Mn(III)Mn(IV) dimer such as that shown in Figure 5C for the bipyridyl Mn compound is not available. In addition, as mentioned above, the ENDOR data on the bipyridyl Mn compound have been interpreted as indicating coupling from the (terminal) ^{14}N donors with $A_{iso} \cong 9$ MHz (Khangulov et al., 1993), whereas an interpretation of the ESEEM data on the same compound yielded $A_{iso} \cong 2.8$ MHz (Britt, 1988). However, the following points are relevant to this question.

It is shown above that the ESEEM data on the methylated catalase are similar to those measured on the model compound with an intense frequency feature at ca. 1.6 MHz and a second peak at ca. 6 MHz. This similarity would suggest that the ^{14}N ligands have hyperfine coupling constants of comparable magnitude in the two systems, i.e., $A_{iso} \cong 9$ MHz. The results of the methylation have been interpreted as indicating that one arm of the amido bridge from the lysine is broken by the methylation procedure, with subsequent methylation of the amine. Thus, the spectroscopic data would suggest that this is accompanied by an increase in the isotropic hyperfine coupling constant of the ^{14}N from $A_{iso} = 2.45$ MHz to $A_{iso} \cong 9.0$ MHz. The magnitude of the hyperfine coupling via an isotropic Fermi contact mechanism is largely dependent on the electron spin density in the 2s valence orbital (Owen & Thornley, 1966; Tan et al. (1991). Tan et al. (1991) have also proposed that the relatively large value of the isotropic hyperfine coupling from the ^{14}N in the two Mn(III)Mn(IV) compounds mentioned above is indicative of an axial nitrogen on the Mn(III) ion, where the electron spin is contained in a σ-antibonding orbital along the Mn(III)−nitrogen bond. The larger isotropic hyperfine coupling constant that could thus be inferred from the ESEEM data would suggest that, in the methylated enzyme, the lysine ^{14}N coordinates the Mn(III) ion in an axial position.

An alternative interpretation of the ESEEM spectra of the Mn−bipyridyl model compound and the methylated catalase is suggested by the following point: Tan et al. (1991) reported poorly resolved lines at frequencies between 1 and 5 MHz in the CW ENDOR spectra for the cyclam and tmpa model compounds. These additional lines could be related to nitrogen couplings with $A_{iso} \cong 2.8$ MHz and thus correspond to the nitrogen nuclei that are detected by ESEEM for the $[Mn_2(bipy)_4(\mu\text{-}O)_2](ClO_4)_3$ model compound (Britt, 1988; this work). However, the present ESEEM data indicate that the regime of exact cancellation is not applicable for the ^{14}N couplings detected in the Mn−bipyridyl compound or for the methylated catalase. In fact, both instances could be treated as large deviations from the exact cancellation limit, in which regime the ESEEM spectrum shows two predominant fundamental frequencies ν_+ and ν_-, defined by:

$$\nu_\pm = 2[\nu_{eff\pm}{}^2 + K^2(3 + \eta^2)]^{1/2}$$

with two additional broader peaks which may be difficult to observe experimentally (Flanagan & Singel, 1987). Taking the frequency values of the most prominent peaks at ca. 2 and 5.5 MHz as $\nu_\pm$ values for the Mn−bipyridyl compound and ca. 1.6 and 6.2 MHz for the methylated catalase, one obtains $A_{iso} = 2.9$ MHz and $A_{iso} = 4.2$ MHz for the isotropic hyperfine coupling terms of the coupled ^{14}N in the model compound and in methylated catalase, respectively. The calculated A_{iso} values fall in the range $A_{iso} > 2\nu(^{14}N)$, which is consistent with the deviation from the cancellation limit. In this interpretation, the additional peaks observed at 2.35 and 3.88 MHz could correspond to the broader peaks predicted by the theory (see above).

In fact, simulations of the ESEEM pattern of the methylated catalase would be needed to extract valuable coupling parameters, especially for the A_{iso} value of the coupled ^{14}N. However, it is of note that both interpretations given above indicate that the methylation of catalase brings a large change in the hyperfine coupling interaction of the ^{14}N.

It has been proposed that an amino ligand derived from the ammonia molecule bridges two Mn ions in Photosystem II inhibited by NH_4Cl (Britt et al., 1989). As mentioned above, the data indicate that the coupling from the ^{14}N satisfies the exact cancellation condition, with the following parameters: $e^2Qq = 1.61$ MHz, $\eta = 0.59$, and $A_{iso} = 2.29$ MHz (Britt et al., 1989). Very similar parameters are extracted from the data reported in this study (see above). For the coupled ^{14}N in the untreated Mn(III)Mn(IV) catalase, it is shown that the regime of exact cancellation is also applicable. The isotropic hyperfine coupling and the asym-

metry parameter of the NQI are similar (A_{iso} = 2.45 MHz, η = 0.51). This strengthens our interpretation for a similar mode of coordination for the ^{14}N in the two systems. The data also indicate that the electric field gradient is 40% larger for the bridging ^{14}N in catalase (e^2Qq = 2.34 MHz). The local structure about the ϵ-amino nitrogen in protonated lysine resembles that of alkyl-substituted ammonium cations, for which e^2Qq values of ca. 0.9 MHz have been measured in the solid state (Hunt & Mackay, 1974). This value is expected to increase significantly upon deprotonation of the amine and binding to the two metal ions. For instance, the amino nitrogen of imidazole has an e^2Qq value of 1.43 MHz, but this increases to 2.82 MHz for the imino nitrogen of imidazole coordinated to a Cd(II) ion (Ashby et al., 1978). Thus, a significant increase from the value in protonated lysine is expected for the e^2Qq of the bridged ^{14}N in Mn(III)Mn(IV) catalase. The difference in the electric field gradients for the coupled ^{14}N in inhibited PSII (e^2Qq = 1.67 MHz) and catalase (e^2Qq = 2.34 MHz) could reflect the electron-donating effect of the alkyl group on the amido bridge in Mn(III)Mn(IV) catalase.

Upon incubation with formaldehyde and cyanoborohydride the CW-EPR and ESEEM spectra of the Mn(III)Mn(IV) catalase are dramatically altered. The spectroscopic data are interpreted as indicating that one arm of the bridging lysine is detached from one Mn ion, resulting in a change from a bridging to a terminal ligation. EPR and ESEEM spectroscopy alone cannot unequivocally address the question of which Mn remains attached to the lysine, since the electronic spin is delocalized over the entire Mn(III)Mn(IV)dimer. However, the following point is relevant to this question: the significant electron spin density on the ^{14}N ligand which is reflected by the relatively large isotropic hyperfine interaction suggests that the metal valence orbital transfers unpaired electron spin in the 2s orbital of the nitrogen. This indicates that the metal orbital that is involved is an e_g orbital. Mn(IV) (d^3) has its three unpaired electrons in three t_{2g} orbitals, but Mn(III) (d^4) has its additional unpaired electron is an e_g orbital (d_{z^2} or $d_{x^2-y^2}$). This reasoning, analogous to that proposed by Tan et al. (1991) to interpret the ^{14}N ENDOR spectra, suggests that in methylated catalase the ^{14}N ligand coordinates to the Mn(III) ion.

The results of the spectral simulations also indicate that the magnetic parameters that best fit the EPR spectra are changed after the methylation procedure. Table 1 shows that the most significant changes in the hyperfine parameters are a 42% increase from $A_{||}$ = 311.8 MHz to $A_{||}$ = 443.7 MHz for the z component of the hyperfine coupling tensor from the Mn(III) ion, together with a 14% decrease in the $A_{||}$ for the Mn(IV) ion. The most dramatic changes seem to be constrained to the parallel components of the hyperfine tensors. Because the corresponding direction is perpendicular to the presumed $Mn_2(\mu\text{-}O)_2$ plane, it is reasonable to conclude that the perturbation brought about by the methylation mainly translates into geometrical changes in the axial ligands to the Mn ions. This strongly suggests that the lysine bridging ligand coordinates the Mn dimer in a position of mostly axial character.

The spectral simulations also indicate that the CW spectrum of the catalase becomes more isotropic after the methylation (Δg = 0.002 vs Δg = 0.018, Table 1). The hyperfine tensor of the Mn(III) ion is significantly more isotropic also (ΔA = 39 MHz vs ΔA = 114 MHz). Upon methylation, the lysine residue changes from a bridging to a nonbridging ligand. This modification in the coordination of the dimeric Mn(III)Mn(IV) core certainly changes the geometry around the Mn ions. Recent data from electronic absorption spectroscopy and MCD have been interpreted as indicating the presence of a bent, tribridged $(\mu\text{-}O)_2$ Mn(III)-Mn(IV) core in Mn(III)Mn(IV) catalase (Gamelin et al., 1994). From previous data from EXAFS spectroscopy, it had been proposed that a possible bridging motif between the two Mn is the di-μ-oxo, μ-carboxylato unit (Waldo et al., 1992). Our data on the Mn(III)Mn(IV) catalase suggest that one of the bridging atoms is a nitrogen. In di-μ-oxo Mn(III)Mn(IV) dimers, the two Mn ions and the two atoms of the bridge form a near-planar geometry. Thus, the loss of the μ-amido bridge upon methylation is expected to bring a more planar configuration for the metal core. Our data indicate that this change in geometry is reflected in the properties of the g-tensor, and perhaps of the ^{55}Mn hyperfine tensors also.

To our knowledge, there is no precedent in the literature of a metal enzyme with a dimeric metal core bridged by the ϵ-amino group from a lysine residue. Compounds of manganese or other transition metal ions with bridging ligands derived from amines can be found in the literature (Chisholm & Rothwell, 1987). For instance, the synthesis and characterization of a Mn(II) dimer with two bis-(trimethylsilyl)amido bridging ligands have been reported (Murray & Power, 1984). More recently, Belforte et al. (1989) have shown that the di-μ-diethylamido bridge mediates antiferromagnetic coupling in a compound with three bridged Mn(II) ions. An interesting and related bridging motif with nitrogen donors is found in Cu(II)Zn(II) superoxide dismutase, the crystal structure of which shows that the two metal ions are bridged by the imidazolate group of a histidine residue (Tainer et al., 1982). In this enzyme, both the N_δ and N_ϵ of the imidazolate are involved in the bridge between the metals, resulting in a μ,η^2 coordination. A similar μ,η^2 imidazolate bridge has been recently suggested to be present in the Mn tetranuclear cluster of Photosystem II (Tang et al., 1994). Here, the proposed bridge from the ϵ-amino group of the lysine would result in a μ,η^1 coordination of the metal core. This does not necessarily mean that this lysine is a ligand (bridging or nonbridging) in the other oxidation states which are found to be formed during catalysis, in particular, Mn(II)Mn(II) and Mn(III)Mn(III). For instance, the lysine residue may be very close to the metal center, and upon oxidation to the Mn(III)Mn(IV) state, the nearby uncharged amino group of the lysine binds to the more acidic Mn dimer. As already shown by Khangulov et al. (1993), the Mn(III)Mn(IV) state is an inactive state, in that the catalase is unable to disproportionate hydrogen peroxide. The present results may be interpreted as indicating that the origin of the inactivation is the irreversible binding of the lysine to the dimanganese center, preventing the peroxide molecule from binding to the metals.

Penner-Hahn (1992) has proposed a mechanistic model for the catalytic cycle of manganese catalase. In this model, the hydroperoxo form of a peroxide molecule binds to the Mn(II)Mn(II) catalase by displacing a water ligand. Reduction of the peroxide by the manganese and deprotonation of a nearby basic amino acid result in the formation of an oxo bridge between the two resultant Mn(III) ions and the release of a water molecule. The Mn(III)Mn(III) dimer then oxidizes

a second peroxide molecule to dioxygen and returns to the Mn(II)Mn(II) oxidation state, with concomitant reprotonation of the basic amino acid. It is possible that the lysine that we have detected in the present study acts as the basic amino acid of the Penner-Hahn model in the low oxidation states that are involved in the catalytic cycle. The ESEEM data reported in the present study provide information on the Mn(III)Mn(IV) state of the enzyme. As mentioned above, oxidation of the Mn dimer to this higher oxidation state may result in the irreversible binding of the deprotonated ϵ-amino group of the lysine to the manganese and block the catalytic cycle of the catalase. Alternatively, it is also possible that the lysine residue is a ligand to the manganese in the lower oxidation states of the enzyme. More work needs to be done to substantiate this possibility.[3]

The three pulse ESEEM data on Mn(III)Mn(IV) catalase are proposed to originate from the coupling of a bound lysine in this oxidation state. There is no indication of other peaks in the Fourier transform shown in Figure 1, that could be assigned to frequencies arising from other coupled ^{14}N nuclei, or from intermodulation bands if more than one ^{14}N were coupled to the Mn spin. Apart from the peak at 14.9 MHz that is resolved at 3500 G, and that arises from weakly coupled protons, no other peak could be observed, even when the ESEEM was measured with other τ values. This is taken as evidence that the lysine is the only nitrogen donor to the metal site in Mn(III)Mn(IV) catalase. It is concluded that the other ligands to the Mn dimer are oxygens from, e.g., carboxylates from glutamic or aspartic acids, or water or hydroxyl groups. On the basis of CW ENDOR data on Mn(III)Mn(IV) catalase, Khangulov et al. (1993) also proposed that the majority of the donors to the Mn were oxygens.

This situation is certainly different from what is found for the Mn cluster in Photosystem II. In this case, a histidine residue was recently demonstrated to be a ligand to the Mn cluster by ESEEM spectroscopy (DeRose et al., 1991; Tang et al., 1994). If the ϵ-amino group of the lysine detected in the present work is still a ligand of the manganese in the active Mn(II)Mn(II) and/or Mn(III)Mn(III) states of the catalase, this difference in the coordination of the manganese ions in the catalase and in Photosystem II may be related to the different chemical reactions catalyzed by these enzymes. Although both are made of clusters of Mn ions, these two catalytic metal sites appear to present rather different coordinations, and these differences may be of more significant importance than has usually been considered.

Results from the amino acid analysis of the enzyme before and after the methylation procedure indicate that 64% of the lysine residues can be methylated, among which is the bridging lysine; this means ca. 13 Lys based on the total number of lysines (21) that is given by the analysis of the amino acid composition of the *T. thermophilus* catalase. This indicates that the bridging lysine and the dimeric metal core are relatively easy to access to by exogenous substrates. A difference in accessibility to the catalytic site of the catalases from *L. plantarum* and *T. thermophilus* has been proposed in connection with the pH dependence of azide inhibition in each species (Penner-Hahn, 1992); it was proposed that the catalytic site of the *T. thermophilus* catalase is directly accessible by solvents while that of *L. plantarum* is only accessible via a hydrophobic channel. It would be interesting to test the sensitivity of the *L. plantarum* catalase to the methylation procedure in order to substantiate this fact.[4]

[3] The refinement of the crystal structure of Mn catalase from *T. thermophilus* is in progress in the laboratory of Dr. Barynin. The results indicate that Lys 194 is very close to the Mn ions. It will be interesting to see in the refined crystal structure if this lysine is actually a ligand to the manganese(s).

ACKNOWLEDGMENT

We thank Drs. Gérard Berger, Hervé Bottin, and Bernard Lagoutte for extremely useful discussions, Dr. Françoise Bouet for performing the amino acid analyses of catalase, and Dr. Paul Mathis for continuous support of this work.

REFERENCES

Allgood, G. S., & Perry, J. J. (1986) *J. Bacteriol. 168*, 563−567.
Ashby, C. I. H., Cheng, C. P., & Brown, T. L. (1978) *J. Am. Chem. Soc. 100*, 6057−6063.
Barynin, V. V., & Grebenko, A. I. (1986) *Dokl. Akad. Nauk SSSR 286*, 461−464.
Barynin, V. V., Vagin, A. A., Melik-Adamyan, V. R., Grebenko, A. I., Khangulov, S. V., Popov, A. N., Andrianova, M. E., & Vainshtein, B. K. (1986) *Dokl. Akad. Nauk SSSR 228*, 877−880 (Russian).
Belforte, A., Calderazzo, F., Englert, U., & Strähle, J. (1989) *J. Chem. Soc., Chem. Commun.*, 801−802.
Berger, G., Mazière, M., Prenant, C., Sastre, J., & Comar, D. (1984) *Int. J. Appl. Radiat. Isot. 35*, 81−83.
Bidlingmeyer B. A., Cohen S. A., & Tarvin T. L. (1984) *J. Chromatogr. 336*, 93−104.
Bonvoisin, J., Blondin, G., Girerd, J. J., & Zimmermann, J. L. (1992) *Biophys. J. 61*, 1076−1086.
Britt, R. D. (1988) Ph.D. Thesis (Lawrence Berkeley Laboratory, Report LBL-25042), Department of Physics, University of California, Berkeley, CA.
Britt, R. D., Zimmermann, J. L., Sauer, K., & Klein, M. P. (1989) *J. Am. Chem. Soc. 111*, 3522−3532.
Cammack, R., Chapman, A., McCracken, J., Cornelius, J. B., Peisach, J., & Weiner, J. H. (1988) *Biochim. Biophys. Acta 956*, 307−312.
Chisholm, M. H., & Rothwell, I. P. (1987) in *Comprehensive Coordination Chemistry* (Wilkinson G., Gillard R. D., & McCleverty, J. A., Eds.) pp 161−188, Pergamon Press, Oxford.
Cooper, S. R., & Calvin, M. (1977) *J. Am. Chem. Soc. 99*, 6623−6630.
Deisseroth, A., & Dounce, A. (1970) *Physiol. Rev. 50*, 319−375.
DeRose, V. J., Yachandra, V. K., McDermott, A. E., Britt, R. D., Sauer, K., & Klein, M. P. (1991) *Biochemistry 30*, 1335−1341.
Dikanov, S. A., Tsvetkov, Y. D., Khangulov, S. V., & Gol'dfel'd, M. G. (1988) *Dokl. Akad. Nauk SSSR 302*, 1255−1257.
Fauth, J. M., Schweiger, A., Braunschweiler, L., Forrer, J., & Ernst, R. (1986) *J. Magn. Reson. 66*, 74−85.
Flanagan, H. L., & Singel, D. J. (1987) *J. Chem. Phys. 87*, 5606−5616.
Fronko, R. M., Penner-Hahn, J. E., & Bender, C. J. (1988) *J. Am. Chem. Soc. 110*, 7554−7555.
Gamelin, D. R., Kirk, M. L., Stemmler, T. L., Pal, S., Armstrong, W. H., Penner-Hahn, J. E., & Solomon, E. I. (1994) *J. Am. Chem. Soc. 116*, 2392−2399.
Haddy, A., Waldo, G. S., Sands, R. H., & Penner-Hahn, J. E. (1994) *Inorg. Chem. 33*, 2677−2682.

[4] Alternative interpretations of the data presented in this paper cannot be completely ruled out. As mentioned by a reviewer, it cannot be excluded that methylation of the lysines in the enzyme causes a conformational change that propagates to the Mn active site, resulting in a change in the EPR and ESEEM properties of the Mn dimer. However, the model of the bridging lysine proposed here provides a suitable interpretation for the peculiar spectroscopic data of Mn catalase and is completely consistent with the current mechanistic model of the enzyme; in our model, it is proposed that the basic residue that assists catalysis is a lysine, and a provisional explanation for the inactivation of the enzyme in the Mn(III)Mn(IV) state is given.

Hunt, M. J., & Mackay, A. L. (1974) *J. Magn. Reson. 15*, 402−414.
Jiang, F., McCracken, J., & Peisach, J. (1990) *J. Am. Chem. Soc. 112*, 9035−9044.
Kevan, L. (1990) in *Modern Pulsed and Continuous-Wave Electron Spin Resonance* (Kevan, L., & Bowman, M. K., Eds.) pp 231−266, Wiley Interscience, New York.
Khangulov, S. V., Barynin, V. V., & Antonyuk-Barynina, S. V. (1990a) *Biochim. Biophys. Acta 1020*, 25−33.
Khangulov, S. V., Barynin, V. V., Voevodskaya, N. V., & Grebenko, A. I. (1990b) *Biochim. Biophys. Acta 1020*, 305−310.
Khangulov, S., Sivaraja, M., Barynin, V. V., & Dismukes, G. C. (1993) *Biochemistry 32*, 4912−4924.
Kono, Y., & Fridovitch, I. (1983) *J. Biol. Chem. 258*, 6015−6019.
Larson, R. G., & Pecoraro, V. L. (1992) in *Manganese Redox Enzymes* (Pecoraro, V. L., Ed.) pp 1−27, VCH Publishers, New York.
LoBrutto, R., Smithers, G. W., Reed, G. H., Orme-Johnson, W. H., Tan, S. L., & Leigh, J. S. (1986) *Biochemistry 25*, 5654−5660.
Means, G. E., & Feeney, R. E. (1968) *Biochemistry 7*, 2192−2201.
Melik-Adamyan, W. R., Barynin, V. V., Vagin, A. A., Borisov, V. V., Vainshtein, B. K., Fita, I., Murthy, M. R. N., & Rossmann, M. G. (1986) *J. Mol. Biol. 188*, 63−72.
Mims, W. B. (1972) *Phys. Rev. 5*, 2409−2419.
Mims, W. B. (1984) *J. Magn. Reson. 59*, 291−306.
Mims, W. B., & Peisach, J. (1978) *J. Chem. Phys. 69*, 4921−4930.
Mims, W. B., & Peisach, J. (1981) in *Biological Magnetic Resonance* (Berliner, L. J., & Reuben, J., Eds.) Vol. 3, Chapter 5, pp 213−263, Plenum Press, New York.
Mims, W. B., & Peisach, J. (1989) in *Advanced EPR, Applications in Biology and Biochemistry* (Hoff, A. J., Ed.) Chapter 1, pp 1−57, Elsevier Science Publishers, Amsterdam.
Murray, B. D., & Power, P. P. (1984) *Inorg. Chem. 23*, 4584−4588.
Murshudov, G. N., Melik-Adamyan, W. R., Grebenko, A. I., Barynin, V. V., Vagin, A. A., Vainshtein, B. K., Dauter, Z., & Wilson, K. S. (1992) *FEBS Lett. 312*, 127−131.
Murthy, M. R. N., Reid, T. J., III, Sicignano, A., Tanaka, N., & Rossman, M. G. (1981) *J. Mol. Biol. 152*, 465−499.
Owen, J., & Thornley, J. H. M. (1966) *Rep. Prog. Phys. 29*, 675−728.
Penner-Hahn, J. E. (1992) in *Manganese Redox Enzymes* (Pecoraro, V. L., Ed.) pp 29−45, VCH Publishers, New York.
Schonbaum, G. R., & Chance, B. (1976) in *The Enzymes* (Boyer, P. D., Ed.) Vol. 13, pp 363−408, Academic Press, New York.
Tainer, J. A., Getzoff, E. D., Beem, K. M., Richardson, J. S., & Richardson, D. C. (1982) *J. Mol. Biol. 160*, 181−217.
Tan, S. L., Fox, J. A., Kojima, N., Walsh, C. T., & Orme-Johnson, W. H. (1984) *J. Am. Chem. Soc. 106*, 3064−3066.
Tan, X.-L., Gultneh, Y., Sarneski, J. E., & Scholes, C. P. (1991) *J. Am. Chem. Soc. 113*, 7853−7858.
Tang, X.-S., Diner, B. A., Larsen, B. S., Gilchrist, M. L., Lorigan, G. A., & Britt, R. D. (1994) *Proc. Natl. Acad. Sci. U.S.A. 91*, 704−708.
Thomann, H., & Bernardo M. (1993) in *Biological Magnetic Resonance* (Berliner, L. J., & Reuben, J., Eds.) Vol. 13, Chapter 7, pp 275−320, Plenum Press, New York.
Vainshtein, B. K., Melik-Adamyan, W. R., Barynin, V. V., Vagin, A. A., & Grebenko, A. I. (1985) *Proc. Int. Symp. Biomol. Struct. Interact. Suppl. J. Biosci. 8*, 471−479.
Waldo, G. S., Yu, S., & Penner-Hahn, J. E. (1992) *J. Am. Chem. Soc. 114*, 5869−5870.
Zheng, M., Khangulov, S. V., Dismukes, G. C., & Barynin, V. V. (1994) *Inorg. Chem. 33*, 382−387.
Zimmermann, J. L., Boussac, A., & Rutherford, A. W. (1993) *Biochemistry 32*, 4831−4841.

BI942235R